

	
Project (Grant) Number:	824135
Project Acronym:	SOLARNET
Project Title:	Integrating High Resolution Solar Physics

Document Details	
Document Title	Simulation Results
Prepared by (Institution's Name):	University of Durham (UDUR)
Work Package (WP) Number & Title	WP7: Multi-Conjugate Adaptive Optics for EST
Deliverable Number & Title:	D7.5 - Simulation Results
Serial Number of Deliverable:	D76
Document Code: (inserted by project office)	D7.5_Version 1.0
File Name: (inserted by project office)	SOLARNET_D7.5_V1.0_SR_Public_20200331
Date Uploaded: (inserted by project office)	March 31 st , 2020

AUTHORS/ CONTRIBUTORS LIST

Name	Function	Organization
Matthew Townson	Scientist and Task leader	UDUR
Alastair Basden	Scientist and Task Contributor	UDUR

SCIENTIFIC APPROVAL CONTROL FROM SUB-WP & WP LEAD

Control	Name	Organization	Function	Date
Prepared	Matthew Townson	UDUR	Task Leader	Mar 20 th , 2020
Prepared	Alastair Basden	UDUR	Task Contributor	Mar 23 rd , 2020
Revised	Matthew Townson	UDUR	Task Leader	Mar 25 th , 2020
Approved	Timothy Morris	UDUR	Sub-WP Leader	Mar 27 th , 2020
Authorized	Oskar von der Lühe	Leibniz Institute for Solar Physics (KIS)	WP Leader	Mar 30 th , 2020

ADMINISTRATIVE APPROVAL CONTROL FROM PROJECT OFFICE

Control	Name	Organization	Function	Date
Approved	Tirtha Som	KIS	Project Manager	Mar 30 th , 2020
Approved	Rolf Schlichenmaier	KIS	Project Coordinator	Mar 31 th , 2020
Authorized	Markus Roth	KIS	Project Scientist	Mar 31 th , 2020

HISTORY OF DOCUMENT CHANGES

Issue	Date	Change Description
Version 1.0	Mar 31 st , 2020	Initial Issue



Table of Contents

List of Abbreviations	4
Simulation Objectives and Summary	5
Proposal	5
Summary of Progress.....	5
DASP	6
DASP-Solar.....	6
Preliminary DASP Results.....	7
Artificial Neural Networks.....	7
MCAO Bench.....	8
Atmospheric Modelling.....	10
References.....	13

List of Abbreviations

ANN	Artificial Neural Network
DARC	Durham Adaptive Optics Real-Time Controller
DASP	Durham Adaptive Optics Simulation Platform
EST	European Solar Telescope
IAC	Instituto de Astrofísica de Canarias
MCAO	Multi-Conjugate Adaptive Optics
PSF	Point Spread Function
SH	Shack-Hartmann
SST	Swedish 1-m Solar Telescope
VTT	Vacuum Tower Telescope
WFE	Wave Front Error
WFS	Wave Front Sensor
WP	Work Package

Simulation Objectives and Summary

Proposal

"The requirements for the EST MCAO system were derived from analytical simulations which were carried out during the EST design study and in earlier projects. These also established approximate conjugate heights for the four DMs and indicate satisfactory compensation for a wide range of elevation angles under favourable seeing conditions. We will carry out further simulations using the Durham Adaptive Optics Simulation Platform (Alastair G. Basden et al. 2007) adapted for solar AO systems (DASP-solar) to establish a complete error budget study using dynamical simulations. We will also use simulations to study the performance of solar MCAO using neural networks for wave front sensing."

Summary of Progress

Since the proposal a number of developments have been made for DASP to make it relevant for solar telescopes and solar AO Systems. These have been applied to two work themes in WP7.

The DASP-Solar simulation has, and continues to, feed into the development of ANN as a possibility for controlling the EST AO system. DASP-Solar is used to simulate a variety of atmospheric conditions at the EST site and simulate an AO system working to correct for these aberrations. The output wide-field SH-WFS images, correlation images, and phase maps produced by DASP-Solar are used in the ANN work. The SH-WFS and correlation images are used as inputs to train the ANN, with over 100,000 individual simulations forming a large training data set. The phase maps simulated by DASP-Solar are used as the validation for the ANN, as the ANN are currently being trained to take the images from a wide-field SH-WFS and produce the corresponding phase which the WFS observes.

The DASP-Solar simulation and the DARC software are being used as part of the development of the MCAO bench hosted by the IAC. DASP and DARC have the ability to communicate between each other, allowing DASP-Solar to simulate hardware which is not physically installed/available on the bench to allow for the development and testing of the AO system whilst components are being installed on the bench.

Simulations of atmospheric statistics are being performed and the spatial statistics compared to the data from wide-field SH-WFS data to better understand and characterise the atmospheric turbulence at the site. This includes matching data taken from the SST (and in future the VTT) to different atmospheric models, such as Kolmogorov statistics. Preliminary results show that the measurements taken by the wide-field SH-WFS data are not completely consistent with Kolmogorov statistics, with further analysis ongoing.

In this report we first describe the capabilities of the DASP-Solar simulation (pg. 6), and then show results of a wavefront reconstruction based on the new Neural network-based wavefront sensing method (pg. 7), and the hardware-in-the-loop MCAO simulation facility (pg. 8). Finally we describe some of the atmospheric modelling work that is being undertaken to better understand the atmospheric turbulence profile and how the AO system controller may be tuned to deal with it (pg. 10).

DASP

DASP is an end-to-end AO simulation package, allowing the exploration of the performance and control methods for AO systems (Alastair G. Basden et al. 2007). The key simulation features offered by DASP include:

- Atmospheric phase screen generation
- Pupil phase generation
- Wavefront sensor simulation
- Centroiding
- Wavefront reconstruction
- PSF generation
- Real-Time Controller Interface (A. G. Basden and Myers 2012; A. Basden et al. 2010)

DASP-Solar

DASP has been expanded to include realistic simulation of extended sources, allowing for the simulation of Solar AO systems (Alastair G. Basden et al. 2018). Simulations from DASP-Solar are required for the ANN work and MCAO bench development, both of which form parts of WP7 and are discussed in detail below.

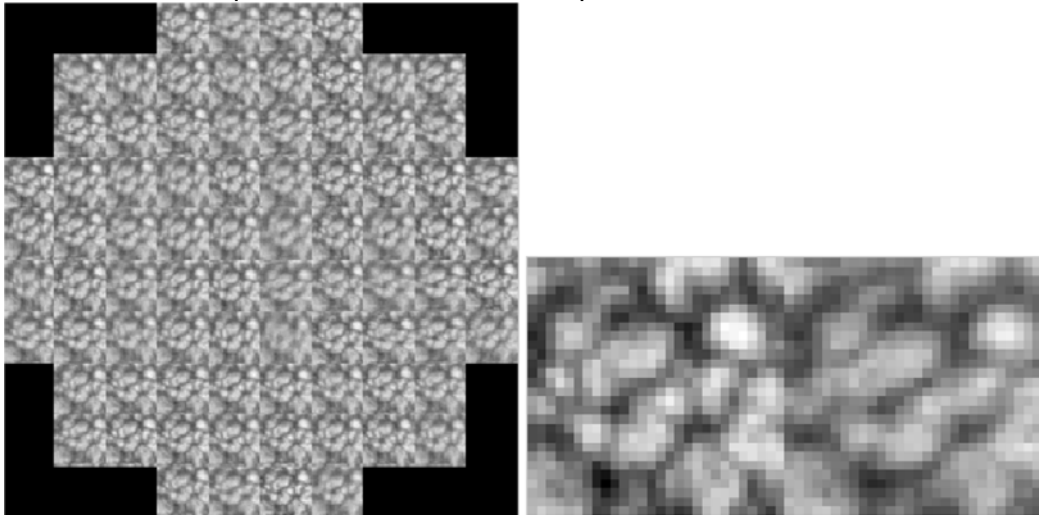


Figure 1: Solar wavefront sensor image from DASP-Solar simulation. Larger views of two sub-apertures are shown on the right showing that DASP-Solar realistically simulates extended sources, including reduction in contrast seen from high altitude atmospheric optical turbulence.

Preliminary DASP Results

Artificial Neural Networks

To date over 100,000 simulations have been run to support the training of ANNs. These simulations cover a variety of different atmospheric conditions, including varying the altitude and strengths of the turbulence simulated. A separate set of ~5000 simulations have been run to generate a validation data set for assessing the performance of the ANNs. The parameters used for a typical training data set are shown in Table 1. A separate training set is created for every source image of the solar structure, or configuration of the telescope.

Parameter	Value
Turbulence Strength (r_0)	8 – 16 cm
Altitude (h)	0 – 20 km
Turbulent layers	2
Image source	Single location of sun
Simulated aberrated Images	90,000

Table 1: Typical configuration of an ANN training data set of simulations.

The outputs of the DASP simulations are the SH-WFS images and the phase map of the turbulence which the light passes through. The SH-WFS images are used as the input to the ANN, and the phase map is used as to validate the output of the ANN. An example single SH-WFS image and corresponding phase map simulated for a 1.5m diameter telescope observing a typical region of solar granulation is shown in Figure 2.

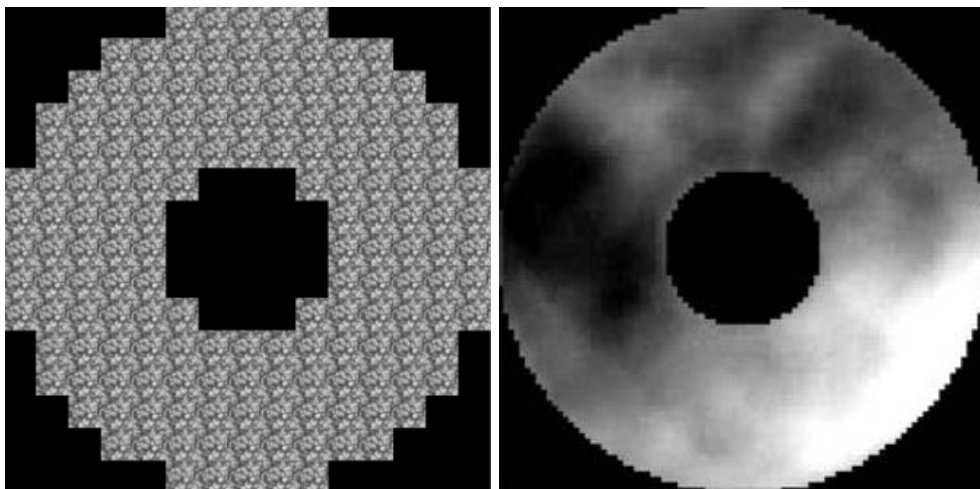


Figure 2: Example output simulated raw SH-WFS image and corresponding phase map

The ANN also includes studying the use of ANNs to perform the wavefront reconstruction step of the AO loop from correlation images generated in the traditional way (Michau, Rousset, and Fontanella 1993). An example output of correlation images and the associated phase map from the DASP simulation is shown in Figure 3.

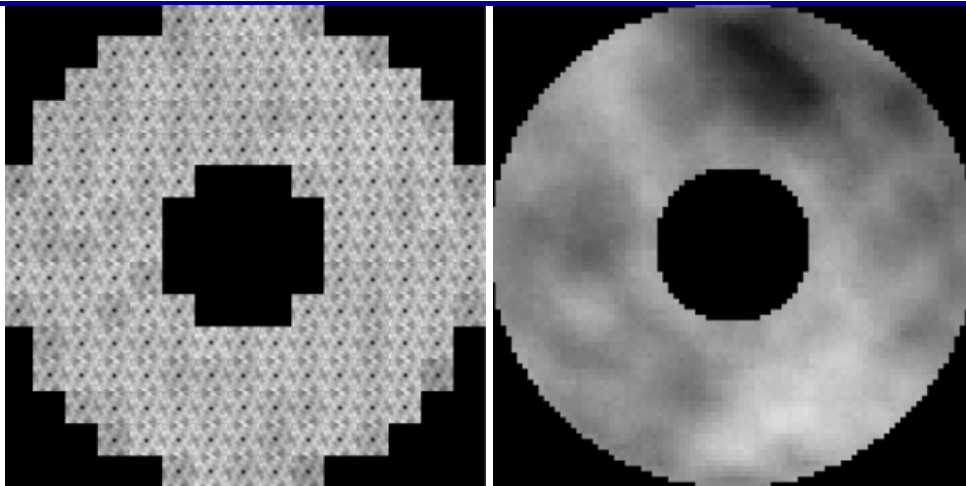


Figure 3: Example output of simulated SH-WFS correlation images and corresponding phase map.

The preliminary results from the ANN trained on the simulation data created so far are shown in Table 2. The residual WFE of the ANN reconstruction method is compared with the obtained by using the standard reconstructions made by DASP based on the SDF cross-correlation algorithm (see Löfdahl 2010 for a full description of the SDF algorithm). The WFE for each case of r_0 is the average over the 3,000 images of each validation dataset.

r_0	Residual Error from ANN		Residual Error from Correlation Images	
	Radians	Nm	Radians	Nm
8	2.14	170.31	2.60	207.20
10	1.82	144.54	2.10	166.98
12	1.52	120.96	1.91	151.99

Table 2: Early results of ANN performance on raw SH-WFS images and correlation images output from DASP.

MCAO Bench

Working with the IAC a model of the EST has been integrated into a hardware-in-the-loop AO simulation facility. This is based on the current likely EST configuration given in Table 3. DASP simulates wide-field images for the configured wide-field SH-WFSs which are then formatted and passed to the real-time control system, which is based on DARC. The real-time control system is configured to receive these images for a TCP/IP socket. The images are calibrated, and then processed using a SDF algorithm to compute wavefront slopes (Löfdahl 2010). The computed slopes are then used to reconstruct the wavefront phase differential introduced by the atmospheric turbulence using a matrix-vector multiplication algorithm.

Parameter	Value
Telescope Diameter	1.5m
Sub-aperture Geometry	15x15
WFS FOV	42"

Table 3: Common simulation configuration. This is representative of a wide-field WFS for the EST.

The reconstructed wavefront phase is used to compute the command vectors to be sent to the deformable mirrors. At this point, the real-time control system sends the DM commands over a TCP/IP socket back to the AO simulation tool, and the loop is completed with the AO simulation using these commands to modify the surface of the simulated DMs.

The AO simulation models the wide-field WFSs by selecting a large number of field directions (typically 36) across the field of view of the WFSs and computing a PSF for each. These PSFs are then convolved by the relevant reference sub-aperture image for this line of sight, and the resulting convolutions combined using a pyramidal hat function. This function gives most weight to the centre of the line of sight, reducing away from it, allowing the strength of signal from the neighbouring lines of sight to become increasingly important.

Control of the hardware-in-the-loop simulations is provided by both the simulation and real-time control components: flux levels, detector noise levels, and other variables dependent on the physical system outside of the real-time control system are controlled using DASP, either by scriptable parameter files used during initialisation of a simulation, or whilst a simulation is running (for example to change the input solar flux) using command line tools or a Python API. Control of the real-time control system is provided using DARC tools. These allow the user to engage the AO loop, to calibrate the system, and to load new reconstruction matrices, loop configurations of wave front sensing parameters.

In this way, the system can be operated as it would be on-sky or on the bench, with a lower frame rate, limited by the computational hardware available to run the simulated hardware elements.

Atmospheric Modelling

As part of other ongoing work in WP7.3 wide-field SH-WFSs are used to collect wavefront slope data from the SST on La Palma. This will be extended to two instruments, one on the SST on La Palma and one on the VTT in Tenerife to allow a comparison of the atmospheric turbulence to feed into the site selection. The geometry of the SH-WFS mapped onto the pupil of the SST is shown in Figure 4.

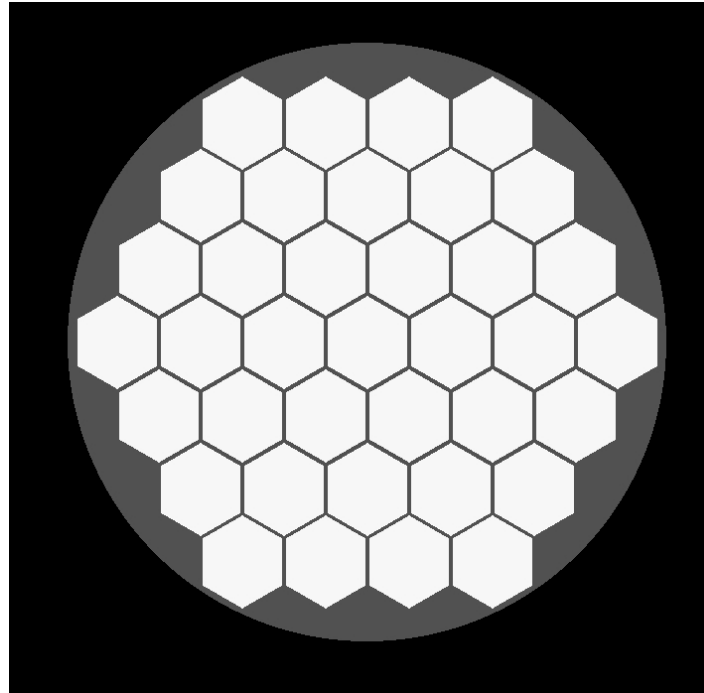


Figure 4: Geometry of Wide-field SH-WFS data across SST pupil.

Data from this instrument will be used to measure the atmospheric turbulence profile for both sites to aid in site selection as part of WP7.3 using the S-DIMM+ technique (Scharmer and van Werkhoven 2010).

The data from these instruments can also be analysed by comparing the motion of different sub-apertures statistically using covariances between sub-apertures similarly to SLODAR in night-time astronomy (Wilson 2002; Butterley, Wilson, and Sarazin 2006). Each sub-aperture in the SH-WFS observes a different cylinder of light from each region of the solar surface. This is illustrated in Figure 5.

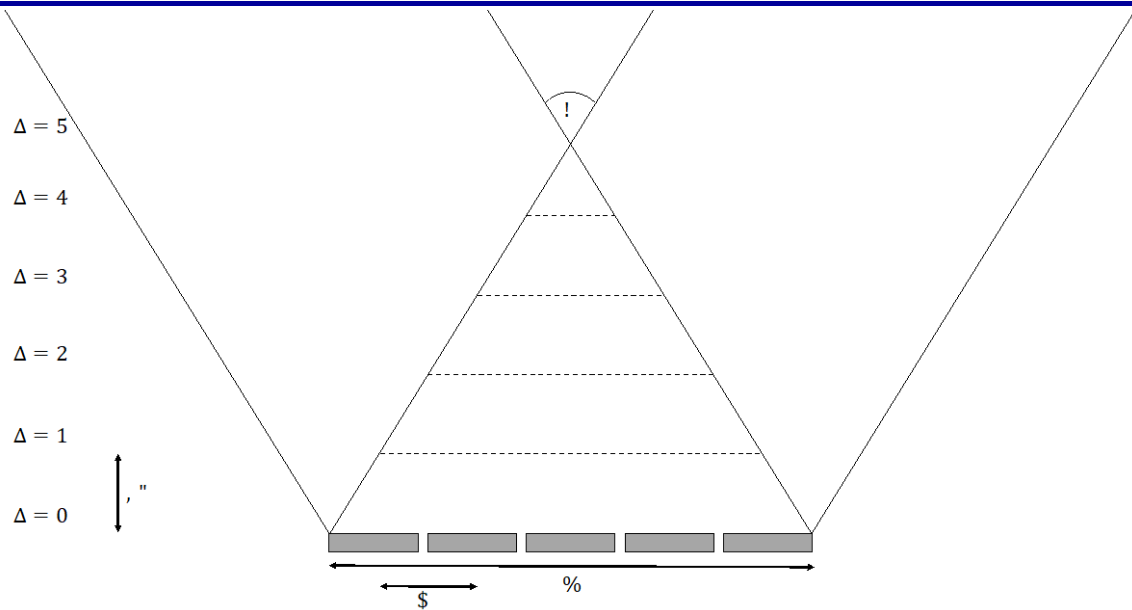


Figure 5: Simplistic diagram showing the sampling of sub-apertures in SH-WFS.

It can be seen from the multiple overlapping cylinders of sampled atmosphere in Figure 5 that multiple altitude regions of the atmosphere are probed at different altitudes, allowing for a profile of the atmospheric turbulence to be calculated. Also, as multiple spatial scales of the turbulence are probed, a measurement of the spatial statistics of the turbulence can be made. This can then be compared to models of atmospheric turbulence, such as Kolmogorov and Von Karman (Kolmogorov 1941; Voitsekhovich 1995). The SLODAR method has been extended to be applicable to wide-field SH-WFS, such as the ones used here in solar astronomy (Townson 2016). The major difference in the technique is the impact of the sub-apertures increasing in effective size with altitude as shown in and described in (Scharmer and van Werkhoven 2010) and Figure 6.

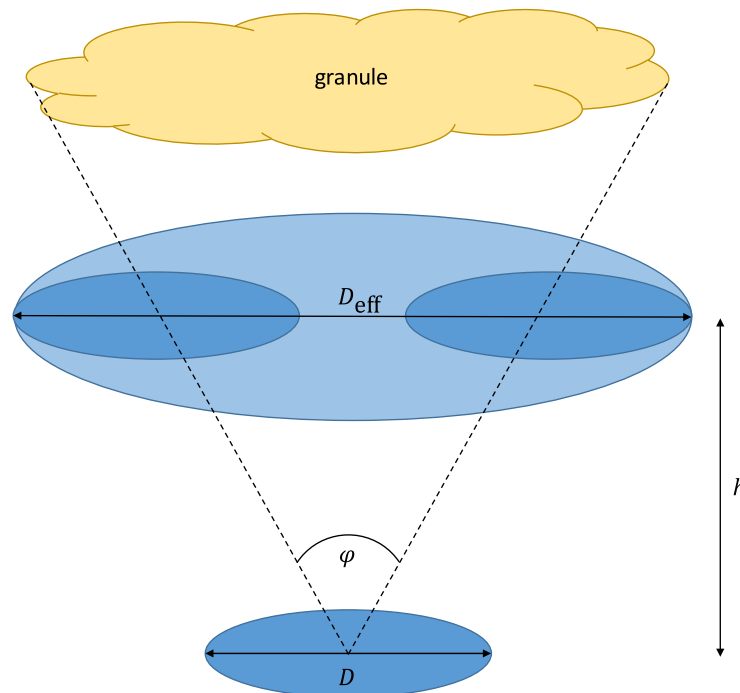


Figure 6: Illustration of increasing size of sub-aperture with altitude.

The sub-aperture diameter, D , effectively increases with altitude as the region used to measure the wavefront gradient is not a point source, but instead extended over an angle, φ .

An example of a measured 1-D spatial-covariance map of the turbulence observed by the wide-field WFS at the SST is shown in Figure 7 and is compared to a similar simulated covariance map using Kolmogorov statistics.

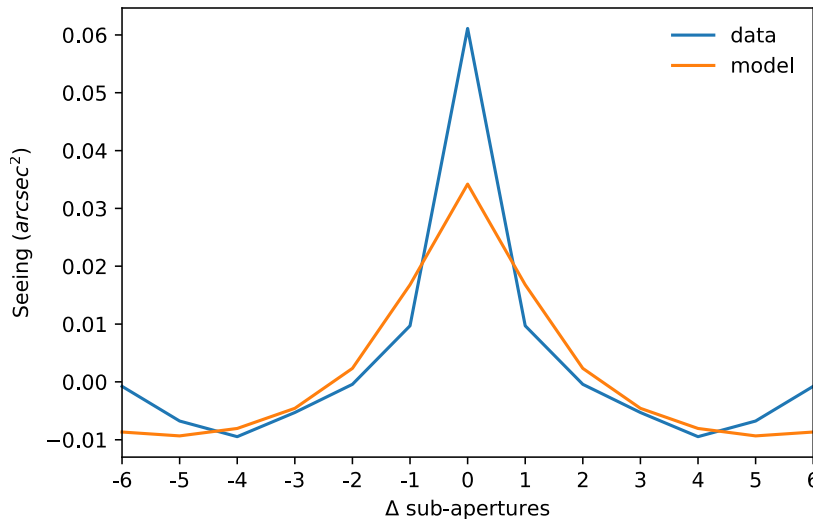


Figure 7: Measured slope covariance and model slope covariance following Kolmogorov statistics.

It is easy to see that the simulated covariance map does not completely agree with the measured covariances. The central point (around a Δ sub-apertures of 0) is subject to noise in the WFS, so is disregarded in the fitting process. However, even without including this data point the “wings” of the two covariance maps have different shapes. This indicates that there may be a difference between that atmospheric statistics that were measured at the site and the atmospheric statistics that have been simulated. The modelling, simulation, and comparison of the wide-field SH WFS data to different atmospheric models is ongoing.

References

- Basden, A. G., and R. M. Myers. 2012. "The Durham Adaptive Optics Real-Time Controller: Capability and Extremely Large Telescope Suitability." *Monthly Notices of the Royal Astronomical Society* 424 (2): 1483–94. <https://doi.org/10.1111/j.1365-2966.2012.21342.x>.
- Basden, Alastair G., N. A. Bharmal, D. Jenkins, T. J. Morris, J. Osborn, J. Peng, and L. Staykov. 2018. "The Durham Adaptive Optics Simulation Platform (DASP): Current Status." *SoftwareX* 7: 63–69. <https://doi.org/10.1016/j.softx.2018.02.005>.
- Basden, Alastair G., Timothy Butterley, Richard Myers, and Richard Wilson. 2007. "Durham Extremely Large Telescope Adaptive Optics Simulation Platform." *Applied Optics* 46 (7): 1089–98. <https://doi.org/10.1364/AO.46.001089>.
- Basden, Alastair, Deli Geng, Richard Myers, and Eddy Younger. 2010. "The Durham Adaptive Optics Real-Time Controller." *Applied Optics* 49 (32): 6354–63. <https://doi.org/10.1364/AO.49.006354>.
- Butterley, Timothy, R. W. Wilson, and M. Sarazin. 2006. "Determination of the Profile of Atmospheric Optical Turbulence Strength from SLODAR Data." *Monthly Notices of the Royal Astronomical Society* 369 (2): 835–45. <https://doi.org/10.1111/j.1365-2966.2006.10337.x>.
- Kolmogorov, a. N. 1941. "The Local Structure of Turbulence in Incompressible Viscous Fluid for Very Large Reynolds Numberst." *Doklady Akademii Nauk Sssr* 30 (1890): 301–5.
- Löfdahl, M. G. 2010. "Evaluation of Image-Shift Measurement Algorithms for Solar Shack-Hartmann Wavefront Sensors." *A & A* 524 (November): A90. <https://doi.org/10.1051/0004-6361/201015331>.
- Michau, Vincent, Gerard Rousset, and J.C. Fontanella. 1993. "Wavefront Sensing of Extended Sources." In *Publication: Real Time and Post Facto Solar Image Correction, Proceedings of the 13th National Solar Observatory/Sacramento Peak Summer Workshop*, 124--8. <http://prints.iiap.res.in/handle/2248/5887>.
- Scharmer, G. B., and T. I. M. van Werkhoven. 2010. "S-DIMM+ Height Characterization of Day-Time Seeing Using Solar Granulation." *A & A* 513 (April): A25. <https://doi.org/10.1051/0004-6361/200913791>.
- Townson, Matthew J. 2016. "Correlation Wavefront Sensing and Turbulence Profiling for Solar Adaptive Optics." Durham University.
- Voitsekhovich, V. V. 1995. "Outer Scale of Turbulence: Comparison of Different Models." *Journal of the Optical Society of America A* 12 (6): 1346. <https://doi.org/10.1364/JOSAA.12.001346>.
- Wilson, R. W. 2002. "SLODAR: Measuring Optical Turbulence Altitude with a Shack-Hartmann Wavefront Sensor." *Monthly Notices of the Royal Astronomical Society* 337 (1): 103–8. <https://doi.org/10.1046/j.1365-8711.2002.05847.x>.